Identification of Two Iron– Chromate Precipitates in a Cr(VI)-Contaminated Soil

ARTICLE *in* ENVIRONMENTAL SCIENCE AND TECHNOLOGY · FEBRUARY 1996

Impact Factor: 5.33 · DOI: 10.1021/es9504348

3 AUTHORS, INCLUDING:

Dirk Baron
California State University, Bakersfield
23 PUBLICATIONS **353** CITATIONS

SEE PROFILE

Identification of Two Iron−Chromate Precipitates in a Cr(VI)-Contaminated Soil

DIRK BARON, CARL D. PALMER,* AND JAMES T. STANLEY

Oregon Graduate Institute of Science & Technology, P.O. Box 91000, Portland, Oregon 97291-1000

Two iron−chromate precipitates, $KFe_3(CrO_4)_2(OH)_6$ (the chromate analog of the sulfate mineral jarosite) and $KFe(CrO_4)_2{\cdot}2H_2O$, were discovered in a soil contaminated by chrome plating solutions. The precipitates were identified by electron microscopy and powder X-ray diffraction. $KFe_3(CrO_4)_2(OH)_6$ was found as small crystals interspersed within the bulk soil. $KFe(CrO_4)_2{\cdot}2H_2O$ forms crusts in cracks and fractures of the soil. Powder X-ray diffraction of the whole soil indicates that most of the Cr(VI) in the soil is present as $KFe_3(CrO_4)_2(OH)_6$ and that the overall amount of $KFe(CrO_4)_2{\cdot}2H_2O$ in the soil is relatively small. The reaction for the transformation between these two phases indicates that $KFe(CrO_4)_2{\cdot}2H_2O$ is likely to form in more acidic , K^+- and $HCrO_4^-$-rich environments than $KFe_3(CrO_4)_2(OH)_6$. Although both of these chromate phases have been synthesized and described, to our knowledge, this study is the first report of their occurrence in the environment.

Introduction

Chromium is a widely used, toxic industrial metal that has been released into the environment at many sites (*1*, *2*). Chromate-laden solutions released into soils by leakage from industrial facilities or by improper waste disposal can alter the chemical environment of soils, resulting in the dissolution of native soil minerals and the precipitation of new phases that incorporate Cr(VI). These precipitates can limit the mobility of Cr(VI) in the subsurface and regulate the bioavailability of Cr(VI). The identification of such precipitates can improve our estimates of the potential risks to human health and the environment at contaminated sites and can greatly contribute to the rational design of remediation systems. In this paper, we report the discovery of two iron chromate precipitates in the soil at a former hard-chrome plating facility.

Experimental Section

Site Description. The United Chrome Products site in Corvallis, OR, is a hard-chrome plating facility that operated between 1956 and 1985. The site is located in the Willamette Valley. Local soils are silt loams of the Amity and Dayton Series (fine-silty, mixed, mesic Argiaquic Xeric Argialbolls and fine, montmorillonitic, mesic Typic Albaqualfs, respectively). Leakage from the plating tanks resulted in the contamination of soil and groundwater. The exact composition of the plating solutions used at this facility is not known. However, in general, hard-chrome plating solutions consist of 1.5−4.5 molar solutions of CrO_3 with a small amount of H_2SO_4 (Cr:S = 80−130:1) (*3*). These solutions are highly acidic with a pH of less than zero. However, the

* Corresponding author telephone: (503) 690-1197; fax: (503) 690-1273; e-mail address: palmer@ese.ogi.edu.

TABLE 1

Comparison of Additional d-Spacings Found in Cr(VI)-Contaminated Whole Soil with d-Spacings Reported by Bonnin and Lecerf (*7*) for Synthetic $KFe_3(CrO_4)_2(OH)_6$

	synthetic $KFe_3(CrO_4)_2(OH)_6$ (*7*)		whole soil	
h, k, l	d-spacing (Å)	rel. int.	d-spacing (Å)	rel. int.
1 0 1	6.04	12	6.02	14
0 0 3	5.82	8	5.82	12
0 1 2	5.18	33	5.16	69
1 1 0	3.715	11	3.71	24
1 0 4	3.617	2		
0 2 1	3.166	100	3.16	100
1 1 3	3.127		3.13	
0 1 5	3.071	1		
2 0 2	3.02	7	3.02	13
0 0 6	2.908	15	2.91	24
0 2 4	2.588	8	2.58	18
1 2 2	2.325	20	2.324	28
0 1 8	2.067	<1		
0 3 3	2.013	25	2.010	23
0 2 7	1.971	3		
0 0 9	1.938	4		
2 2 0	1.858	24	1.852	20
2 0 8	1.805	<1		
2 2 3	1.770	<1		
3 1 2	1.750	5	1.746	4
2 1 7	1.741		1.740	6
1 1 9	1.720	4	1.720	7
1 3 4	1.652	2		
1 2 8	1.624	4	1.621	5
4 0 1	1.6013	5	1.601	4
3 1 5	1.5871	6	1.571	4
0 4 2	1.5788		1.564	9

TABLE 2

Comparison of d-Spacings from Crusts in Soil Fractures with d-Spacings Reported by Bonnin (*6*) for Synthetic $KFe(CrO_4)_2{\cdot}2H_2O$[a]

	synthetic $KFe(CrO_4)_2{\cdot}2H_2O$ (*6*)		crusts in fractures	
h, k, l	d-spacing (Å)	rel. int.	d-spacing (Å)	rel. int.
$2\,0\,\bar{1}$	5.17	s	5.16	88
$2\,0\,\bar{2}$	4.95	s	4.95	78
$1\,1\,\bar{2}$	3.63	s	3.63	78
$2\,0\,\bar{3}$	3.42	w	3.42	34
1 1 1	3.13	vs	3.13	100
$3\,1\,\bar{2}$	3.02	m	3.02	31
$3\,1\,\bar{3}$	2.83	m	2.84	44
0 2 0	2.75	m	2.75	75
$3\,1\,\bar{1}$	2.71	m	2.72	31
$4\,0\,\bar{3}$				
$1\,1\,\bar{3}$	2.584	w	2.58	22

[a] Abbreviations: vs, strongest peak; s, strong peak; m, medium peak; and w, weak peak.

0013-936X/96/0930-0964$12.00/0

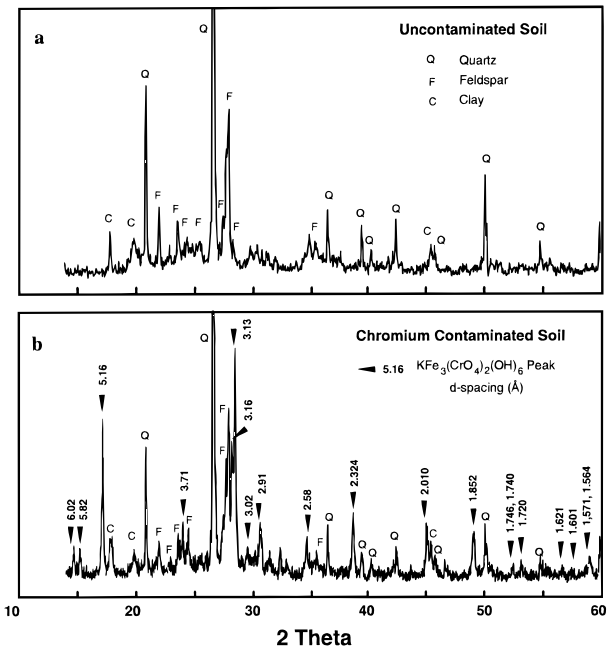

FIGURE 1. Powder X-ray diffraction spectra of (a) uncontaminated background soil and (b) chromium-contaminated soil. The additional peaks in the contaminated soil indicate the presence of a large amount of $KFe_3(CrO_4)_2(OH)_6$.

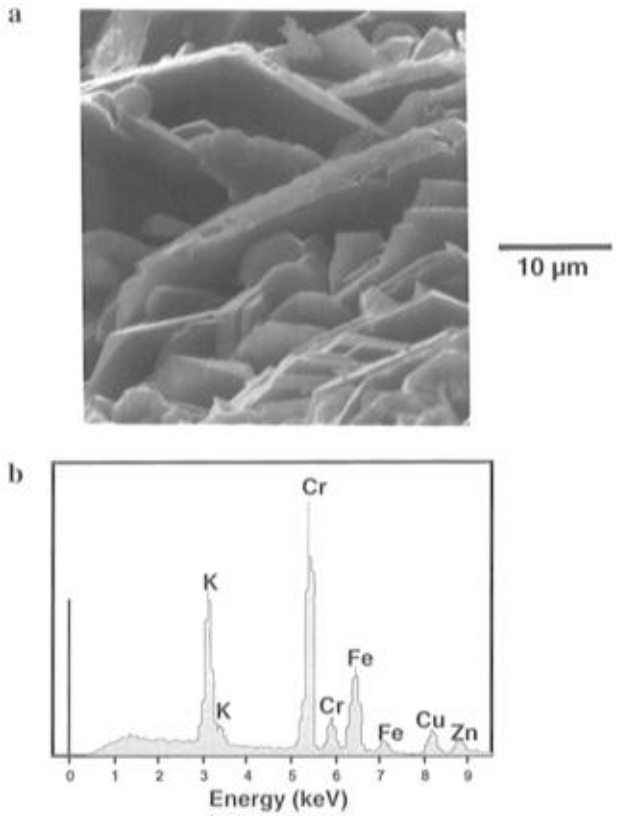

FIGURE 2. Scanning electron micrograph with energy dispersive X-ray spectrum of chromium-containing crystals from crusts precipitated in soil fractures. The crystals were identified as $KFe(CrO_4)_2 \cdot 2H_2O$; Cu and Zn peaks contributed by the sample holder.

pH in the groundwater under the plating tanks was generally around 4, and the lowest measured pH value was 2.3 (*4*). Reported concentrations of hexavalent chromium in the groundwater were as great as 19 000 mg/L (19 g/L). Soils contained as much as 60 000 mg/kg (6%) chromium (*5*). In

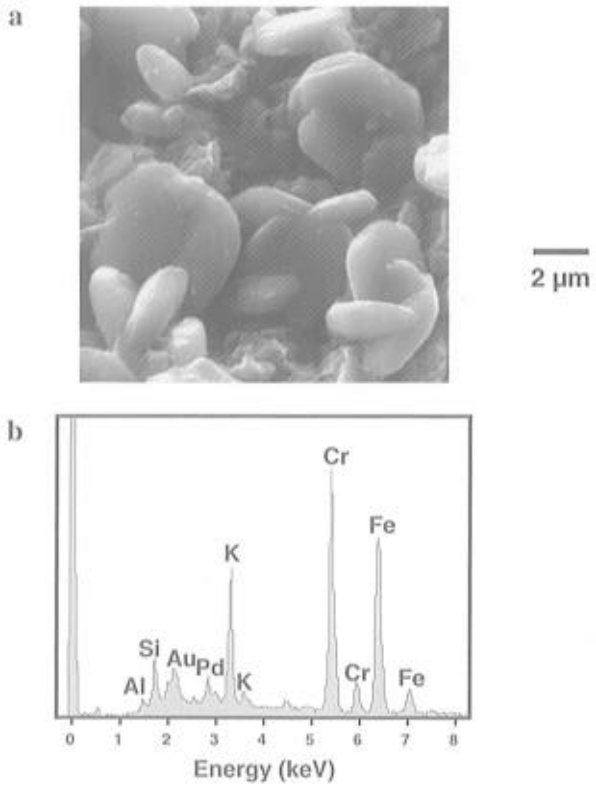

FIGURE 3. Scanning electron micrograph with energy dispersive X-ray spectrum of chromium-containing crystals in the bulk soil. The crystals were identified as $KFe_3(CrO_4)_2(OH)_6$. Si and Al peaks were attributed to the surrounding aluminosilicates; Au and Pd peaks are from the sample coating.

1988, the plating tanks were removed, and underlying soils that had a purple appearance (Munsell color 5RP 2/2) were exposed. Closer examination also revealed crusts of small crystals precipitated in fractures in the discolored soil. When these crystals were ground, they appeared red (Munsell color 2.5 YR 4/6). A background soil sample was taken about 100 m upgradient of the contaminated area for comparison. The background soil sample was chemically analyzed and found to be uncontaminated.

Methods. Whole soil samples for powder X-ray diffraction (XRD) analysis were air-dried and ground in a mortar for 30 min and then analyzed without additional preparation with a Nicolet I2 diffractometer. For the uncontaminated soil the stepsize was 0.05° 2θ and the sampling time was 2 s; for the chromium contaminated soil, the step size was 0.02° 2θ and the sampling time was 5 s. The crystalline crusts that precipitated in soil fractures were separated from the rest of the soil and crushed to obtain a fine powder and analyzed using a Siemens D5000 diffractometer. To allow analysis of the very small amount of sample that was available, a zero background plate, consisting of a single crystal quartz plate mounted in a supporting frame, was used as a sample holder. Stepsize was 0.025° 2θ and the sampling time was 1 s.

The contaminated soil and the crusts were examined under a Zeiss 960 Digital scanning electron microscope (SEM) with a link energy dispersive X-ray spectrometer (EDS). Samples for scanning electron microscopy were air-dried and mounted with carbon. The samples were initially coated with carbon (~400 Å). Samples of the bulk soil were later coated with Au−Pd (~200 Å) to reduce

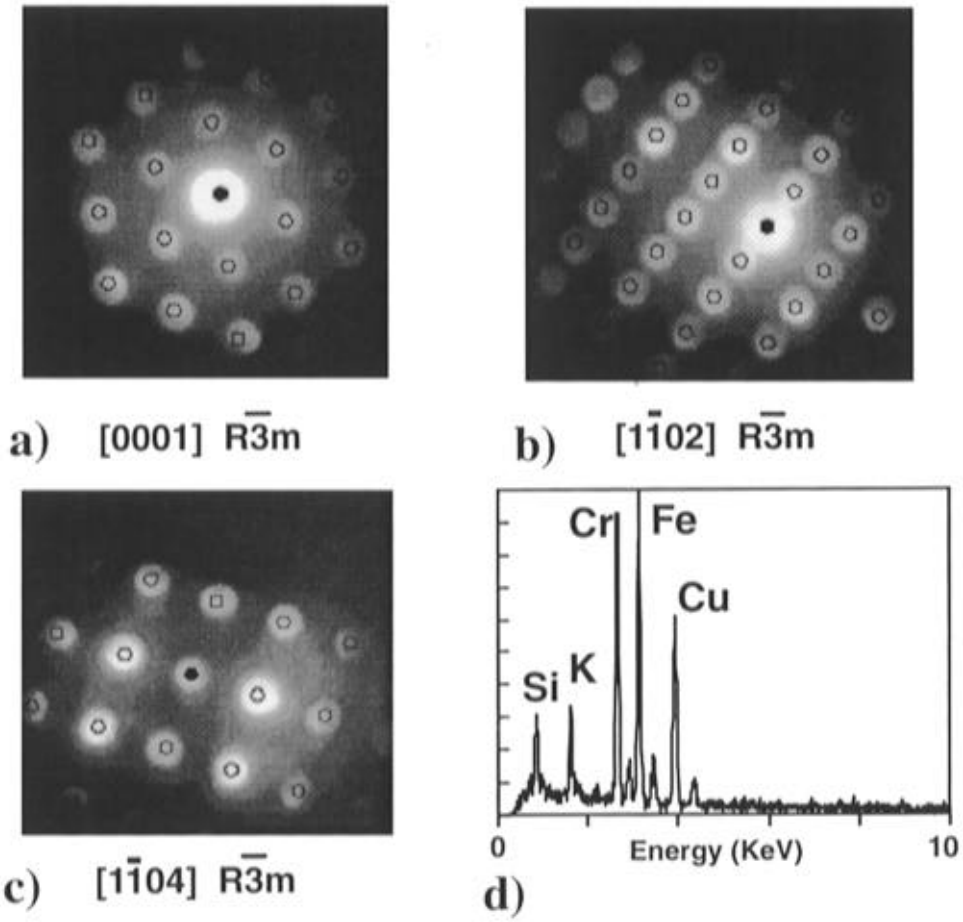

FIGURE 4. TEM electron diffraction patterns and EDS spectrum of $KFe_3(CrO_4)_2(OH)_6$ crystals found in the contaminated soil. (a–c) Electron diffraction patterns; circles superimposed over the electron diffraction patterns are the theoretical patterns for $KFe_3(CrO_4)_2(OH)_6$. (d) EDS spectrum; Si peak was attributed to surrounding silicates; Cu peaks are from the brass specimen holder.

charging. EDS spectra were obtained at a 31 mm working distance with an accelerating voltage of 20 kV with no window.

Samples for transmission electron microscopy (TEM) were prepared by sprinkling small amounts of the sample on copper grids. The samples were examined under a Hitachi 800 TEM/STEM (scanning transmission electron microscope) with a 200-kV accelerator voltage and fitted with a Noran EDS detector and a 5500 Noran analyzer. Selected Area Diffraction (SAD) and convergent beam electron diffraction (CBED) patterns of individual crystals were obtained.

Results

To identify possible chromium precipitates in the Cr(VI)-contaminated soil, a sample of the purple soil was analyzed by powder X-ray diffraction (XRD) and compared to uncontaminated background soil (Figure 1). The major minerals in the uncontaminated soil are quartz, feldspar (labradorite), and clay. In general, powder X-ray diffraction allows the identification of crystalline phases that make up more than about 5–10% of the soil. Minor soil constituents and amorphous phases cannot be detected by XRD of a whole soil sample. Therefore, this XRD scan does not rule out the presence of other minor soil constituents such as iron oxides and hydroxides. The chromium contaminated soil shows additional peaks with the greatest intensities occurring at 3.13, 3.16, and 5.17 Å. These d-spacings are consistent with $KFe_3(CrO_4)_2(OH)_6$, the chromate analog of the sulfate mineral jarosite (*6–10*). Comparison of the additional peaks found in the contaminated soil with the d-spacings and corresponding intensities reported for $KFe_3(CrO_4)_2(OH)_6$ (*7*) (Table 1) clearly demonstrate an excellent match.

The soil was then examined using scanning electron microscopy with energy dispersive X-ray spectroscopy (EDS) to determine if the composition of the crystals is consistent with $KFe_3(CrO_4)_2(OH)_6$ and to ascertain if other chromium-containing phases were present. The crusts in fractures in the soil consist of 10–50 μm, well-formed platy crystals containing K, Fe, and Cr (Figure 2). Small (~2–5 μm) K–Fe–Cr-containing crystals were also found interspersed within the bulk soil (Figure 3). The Fe/Cr ratios from the EDS spectra for the small crystals are 2.8 times greater than the ratios for the larger crystals, indicating that these crystals contain a larger amount of Fe relative to Cr and K.

To determine if the K–Fe–Cr-containing crystals in the crust are structurally different from those in the bulk soil, electron diffraction patterns from single crystals were obtained under the transmission electron microscope. Patterns from crystals found within the bulk soil identify these as rhombohedral (hexagonal), space group R$\bar{3}$m, and confirmed the identification as the chromate analog of jarosite (Figure 4). The crystals found in the soil fractures are monoclinic, space group C2/m, consistent with $KFe(CrO_4)_2 \cdot 2H_2O$ (*6, 11, 12*) (Figure 5). To assure that the individual crystals of $KFe(CrO_4)_2 \cdot 2H_2O$ identified under the TEM were representative of the crusts and not rare

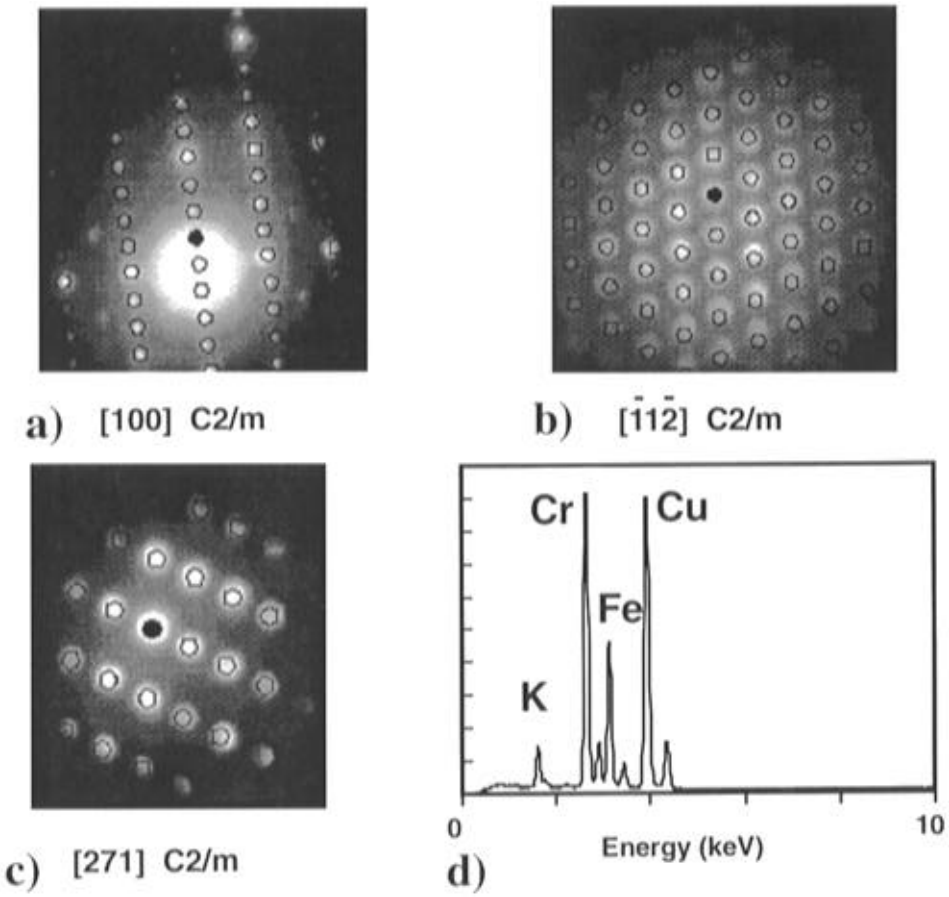

FIGURE 5. TEM electron diffraction patterns and EDS spectrum of $KFe(CrO_4)_2 \cdot 2H_2O$ crystals precipitated in soil fractures. (a–c) Electron diffraction patterns; circles superimposed over the electron diffraction patterns are the theoretical patterns for $KFe(CrO_4)_2 \cdot 2H_2O$. (d) EDS spectrum, the Cu peaks are from the brass specimen holder.

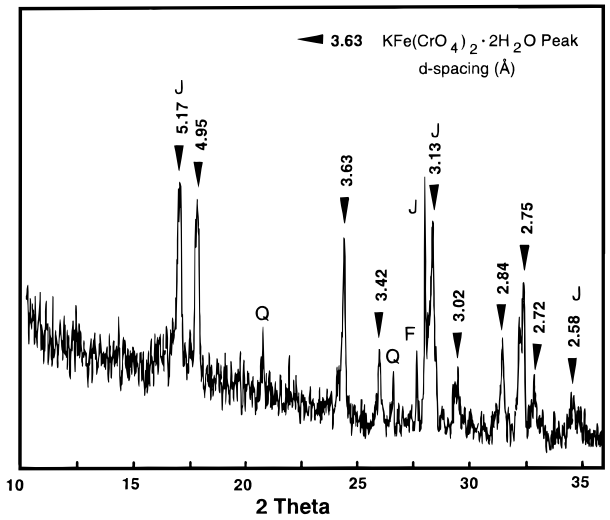

FIGURE 6. Powder X-ray diffraction spectrum of crystals precipitated in soil fractures. Peaks associated with $KFe(CrO_4)_2 \cdot 2H_2O$ are marked with corresponding d-spacings. Peaks corresponding to $KFe_3(CrO_4)_2(OH)_6$ (J), quartz (Q), and feldspar (F) are also marked. The $KFe(CrO_4)_2 \cdot 2H_2O$ peaks for the d-spacings of 3.13 and 5.16 Å coincide with $KFe_3(CrO_4)_2(OH)_6$ peaks.

occurrences in the soil, we obtained an XRD spectrum of the surface crusts. The crusts were carefully scrapped from the soil onto a zero-background plate to try to minimize the amount of underlying soil in the subsample. The XRD scan (Figure 6) yielded $KFe_3(CrO_4)_2(OH)_6$ peaks as well as weaker peaks corresponding to quartz and feldspar. In addition, there are 10 peaks (Table 2) matching very well with the d-spacings and corresponding intensities reported by Bonnin (*6*) for $KFe(CrO_4)_2 \cdot 2H_2O$. Four of the $KFe(CrO_4)_2 \cdot 2H_2O$ peaks (d-spacings 5.17, 3.13, 3.02, and 2.58 Å) are overlain by $KFe_3(CrO_4)_2(OH)_6$ peaks. The 2.75-Å peak from the crusts has a greater intensity than expected from the data for the synthetic $KFe(CrO_4)_2 \cdot 2H_2O$. Although traces of the underlying bulk soil were present in the sample for XRD analysis, the XRD scan confirms that the crusts are composed primarily of $KFe(CrO_4)_2 \cdot 2H_2O$.

Discussion

$KFe_3(CrO_4)_2(OH)_6$ is the structural analog of jarosite ($KFe_3(SO_4)_2(OH)_6$), a mineral that commonly occurs in acid sulfate soils (*13, 14*) and acid mine drainage (*15, 16*). We are not aware of any naturally occurring sulfate analog to $KFe(CrO_4)_2 \cdot 2H_2O$. Although both of these chromate phases have been synthesized and described (*6–12*), to our knowledge this study is the first reported identification in the environment. Although two ferric chromate phases are present in the contaminated soil, the absence of $KFe(CrO_4)_2 \cdot 2H_2O$ peaks in the XRD of the whole soil indicates that most of the Cr(VI) has precipitated as the chromate analog of jarosite. $KFe(CrO_4)_2 \cdot 2H_2O$ is found only in fractures, the preferred flow paths within the saturated soil.

There are no published thermodynamic data for either the chromate analog of jarosite nor $KFe(CrO_4)_2 \cdot 2H_2O$ that we can use to constrain the conditions under which they are likely to form. However, the occurrence of the chromate analog of jarosite in an acid–chromate environment is consistent with the common occurrence of jarosite in acid–

sulfate environments. Assuming that all the available Fe(III) in the soil is bound by these chromate phases, the conversion of $KFe_3(CrO_4)_2(OH)_6$ to $KFe(CrO_4)_2 \cdot 2H_2O$ by

$$KFe_3(CrO_4)_2(OH)_6 + 2K^+ + 2H^+ + 4HCrO_4^- \rightleftarrows 3KFe(CrO_4)_2 \cdot 2H_2O \quad (1)$$

indicates that $KFe(CrO_4)_2 \cdot 2H_2O$ forms in more acidic, more Cr(VI)-enriched waters than those in which $KFe_3(CrO_4)_2(OH)_6$ is stable. As acidic plating solutions entered the subsurface along preferred pathways, $KFe(CrO_4)_2 \cdot 2H_2O$ was the phase initially precipitated from the contaminated groundwater. Cr(VI) and H^+ were primarily from the plating solutions. K^+ was derived from both the plating solution and as an exchangeable cation from the native soil. Fe(III) could have been derived from steel corrosion products in the plating solutions or obtained from naturally occurring iron oxides and hydroxides within the native soil. Although the XRD scan of the soil did not identify iron (oxy)hydroxides as one of the major soil constituents, ammonium oxalate and dithionate, citrate, and bicarbonate (DCB) extractions indicate that the soil contains about 0.004 mg/g of iron as amorphous hydroxides and about 3 mg/g of iron as crystalline oxides and hydroxides (*17*). As the remaining solutes in the contaminated groundwater migrated farther into the sediments, the pH continued to increase due to dilution and the buffer intensity of the soil. Eventually, Cr(VI) and H^+ concentrations decreased to a level where the chromate analog of jarosite became the stable phase. This hypothesis is consistent with the observed spatial distribution of the phases in the soil, the increasing pH with distance from the source, the high Cr(VI) concentrations, and the low Fe concentration observed even in the most acidic waters.

The potential impact of these iron chromate phases on Cr(VI) mobility and the remediation of Cr(VI)-contaminated soil is difficult to assess at this time. Key parameters that are needed include solubility data, the quantity of each phase within the soil, and the time scales for the precipitation and dissolution of these phases. A further complicating factor is the potential formation of solid solutions, particularly with sulfate. Sulfate is a common groundwater constituent and is present in the plating solutions. The equivalent charge, similar structure, and comparable thermochemical radii of chromate and sulfate suggest that solid solutions between these ferric chromate phases and their sulfate analogues could also form. The aqueous Cr(VI) concentrations in solutions equilibrated with such solid solutions could be dramatically different from concentrations in solutions equilibrated with the pure chromate phases.

Summary and Conclusions

Two ferric chromate precipitates were identified in the chromium-contaminated soil. $KFe_3(CrO_4)_2(OH)_6$ was found as small crystals interspersed within the bulk soil. $KFe(CrO_4)_2 \cdot 2H_2O$ forms crusts in cracks and fractures of the soil. The discovery of these ferric chromate phases is a key step in identifying relevant geochemical processes that affect Cr(VI) mobility and impact proposed cleanup operations. Thermodynamic and kinetic studies are needed to determine the potential effect of these phases on the mobility of Cr(VI) in the subsurface. Ultimately, these results should aid in the rational design of cost-effective remediation of chromate-contaminated soils, sediments, and groundwater.

Acknowledgments

This work was supported by the U.S. Environmental Protection Agency, R. S. Kerr Environmental Research Laboratory, Ada, OK. It has not been reviewed by the Agency and does not necessarily reflect their views. We would like to thank Professor André Lecerf of the Laboratoire de Chimie des Matériaux Inorganiques et de Cristallographie, Institut National des Sciences Appliquées, Rennes, France, for providing the powder X-ray diffraction data for synthetic $KFe(CrO_4)_2 \cdot 2H_2O$ and Mr. Scott McKinley from CH2M Hill, Corvallis, OR, for reviewing an earlier version of this manuscript.

Literature Cited

(1) Calder, L. M. In *Chromium in the Natural and Human Environments;* Nriagu, J. O., Nieboer, E., Eds.; John Wiley and Sons: New York, 1988; pp 215−230.
(2) Palmer, C. D.; Wittbrodt, P. R. *Environ. Health Perspect.* **1991**, *92*, 25−40.
(3) Fernald, E. H. In *Metal Finishing, Guidebook Directory Issue '84*; Metals and Plastics Publication, Inc.: Hackensack, NJ, 1984; pp 200−210.
(4) *Deep Aquifer Data Report, United Chrome Products Site, Corvallis, Oregon*; CH2M Hill: Corvallis, OR, 1990.
(5) McKinley, W. S.; Pratt, R. C.; McPhillips, L. C. *Civ. Eng.* **1992**, *62*, 69−71.
(6) Bonnin, A. Ph.D. Dissertation, University of Rennes, France, 1970.
(7) Bonnin, A.; Lecerf, A. *C. R. Seances Acad. Sci. Paris, Ser. C* **1966**, *262*, 1782−1784.
(8) Powers, D. A.; Rossman, G. R.; Schugar, H. J.; Gray, H. B. *J. Solid State Chem.* **1975**, *13*, 1−13.
(9) Cudennec, Y.; Riou, A.; Bonnin, A.; Caillet, P. *Rev. Chim. Miner.* **1980**, *17*, 158−167.
(10) Townsend, M. G.; Longworth, G.; Roudaut, E. *Phys. Rev. B* **1986**, *33*, 4919−4926.
(11) Gravereau, P.; Hardy, A. *Acta Crystallogr. B* **1972**, *28*, 2333−2337.
(12) Mellier, A.; Gravereau, P. *C. R. Seances Acad. Sci. Paris, Ser. B* **1972**, *274*, 1024−1027.
(13) Wagner, D. P.; Fanning, D. S.; Foss, J. E.; Patterson, M. S.; Snow, P. A. In *Acid Sulfate Weathering*; Kittrick, J. A., Ed.; Special Publication No. 10; Soil Science Society of America: Madison, WI, 1982; pp 109−125.
(14) Carson, C. D.; Dixon, J. B. *Soil Sci. Soc. Am. J.* **1983**, *47*, 828−833.
(15) Chapman, B. M.; Jones, D. R.; Jung, R. F. *Geochim. Cosmochim. Acta* **1983**, *47*, 1957−1973.
(16) Alpers, C. N.; Nordstrom, D. K.; Ball, J. W. *Sci. Geol. Bull.* **1989**, *42*, 281−298.
(17) Palmer, C. D.; Wittbrodt, P. R. In *Stage 2 Deep Aquifer Drilling Technical Report, United Chrome Products Site, Corvallis, OR*; CH2M-Hill: Corvallis, OR, Sep 28, 1990.

Received for review June 22, 1995. Revised manuscript received October 2, 1995. Accepted October 2, 1995.[⊗]

ES9504348

[⊗] Abstract published in *Advance ACS Abstracts,* December 15, 1995.